Electronic Selection Rules Controlling Dislocation Glide in bcc Metals

Travis E. Jones,[1,*] Mark E. Eberhart,[2,+] Dennis P. Clougherty,[1,2] and Chris Woodward[3]

[1]*Molecular Theory Group, Colorado School of Mines, Golden, Colorado 80401, USA*
[2]*Department of Physics, University of Vermont, Burlington, Vermont 05405-0125, USA*
[3]*Materials and Manufacturing Directorate, Air Force Research Laboratories, Wright Patterson Air Force Base, Dayton, Ohio 45433-7817, USA*

(Received 5 June 2008; published 21 August 2008)

The validity of the structure-property relationships governing the low-temperature deformation behavior of many bcc metals was brought into question with recent *ab initio* density functional studies of isolated screw dislocations in Mo and Ta. These relationships were semiclassical in nature, having grown from atomistic investigations of the deformation properties of the group V and VI transition metals. We find that the correct form for these structure-property relationships is fully quantum mechanical, involving the coupling of electronic states with the strain field at the core of long $a/2\langle 111\rangle$ screw dislocations.

DOI: 10.1103/PhysRevLett.101.085505 PACS numbers: 61.72.Lk, 71.15.−m

Single crystal bcc metals show remarkable variation in their plastic anisotropy and glide properties. For example, the anisotropy ratio of Ta is twice that of Mo, and under antitwinning stress, Ta is characterized by anomalous glide along {112} planes. This variability must be rooted in the dislocations that mediate plastic behavior. In the case of bcc metals, where the edge and mixed character dislocations are mobile even in the elastic regime, it is the long screw character $a/2\langle 111\rangle$ dislocations that are activated during plastic deformation. Hence, it is differences in the structure of these dislocations that was suspected to be responsible for the variations in plastic anisotropy and glide response of the bcc metals [1,2].

Atomistic calculations designed to elucidate the core structure of $a/2\langle 111\rangle$ dislocations [1,3–5] showed differences between the core structures of Mo and Ta. While the dislocation core of both metals was spread on three conjugate (110) planes, in Ta the spreading was symmetrical about the dislocation line, and for Mo it was asymmetric. Thus, the dislocation core of Ta was characterized by full $D3$ symmetry and Mo by an approximate threefold rotation axis, ($C3$).

Beigi and Arias [6] were the first to question this assumption. Using electronic structure density functional theory (DFT) calculations to study closely spaced dislocation dipole arrays, they found qualitative evidence of symmetric strain fields around $a/2\langle 111\rangle$ screw dislocations in Mo. More realistic and quantitative DFT studies [2,7,8] employing a flexible boundary condition also showed both Mo and Ta to be characterized by symmetric dislocation cores. Further, the calculated anisotropy ratio agreed with the limited experimental measurements, with a twinning-antitwinning asymmetry ratio of 2 in Mo and 4 in Ta.

Despite the computational successes, the underlying structure(s) mediating the deformation properties of bcc metals remain elusive. Here, we show that the variations in glide properties at temperatures where thermally activated dislocation motion is negligible are due to differences in the symmetry imposed coupling between electronic states and applied strain. The selection rules governing this coupling are mediated by the topology of the total charge density at the cores of $a/2\langle 111\rangle$ screw dislocations. It is because Mo has one more valence electron than does Ta, that their charge density topologies, and consequent properties, are also different. (Though the variations in plastic anisotropy are also rooted in differences in electron count and charge density topology, this topic will be saved for a subsequent paper.)

The relationship between charge density topology and mechanical properties can be understood from the Hohenberg-Kohn theorem, which asserts that a system's ground-state properties are a consequence of its charge density, a scalar field denoted as $\rho(\vec{r})$ [9]. Bader [10] noted that the essence of a molecule's structure must be contained within the topology of $\rho(\vec{r})$. The topology of a scalar field is given in terms of its critical points (CPs), which are the zeros of the gradient of this field. There are four kinds of CP in a three-dimensional space: a local minimum, a local maximum and two kinds of saddle point. These CPs are denoted by an index, which is the number of positive curvatures minus the number of negative curvatures. For example, a minimum CP has positive curvature in three orthogonal directions; therefore it is called a (3, 3) CP. The first number is simply the number of dimensions of the space, and the second number is the net number of positive curvatures. A maximum is denoted by (3, −3), since all three curvatures are negative. A saddle point with two of the three curvatures negative is denoted (3, −1), while the other saddle point is a (3, 1) CP. For the purposes of this paper, only the (3, −3) and (3, −1) CPs need further consideration.

Through extensive studies of molecules and crystals, Bader and Zou [11] and Bader [10] showed that it was possible to correlate topological properties of the charge

density with elements of molecular structure and bonding. A maximum, a $(3, -3)$ CP, is always found to coincide with the atomic nucleus, and so is called an atom CP. A bond path was defined to be the ridge of maximum charge density connecting two nuclei such that the density along this path is a maximum with respect to any neighboring path. Bader showed that these ridges correlate with the locations of chemical bonds, leading one to associate the topologically unambiguous bond path with the sometimes subjective chemical bond. The existence of a bond path is guaranteed by the presence of a $(3, -1)$ CP between nuclei. As such, this critical point is often referred to as a bond CP.

With a rigorous description of a bond path as a topological link, it is now possible to identify the bonds between atoms at dislocation cores. Using the charge densities of Reference [5], the bulk topologies of both Ta and Mo were found to be those typical of bcc metals, with eight bond paths to first neighbors (there are no second or higher neighbor bond paths). However, the topological structures of the two equilibrium dislocation cores are distinct (see Fig. 1). Of importance is the recognition that bond paths cross the dislocation core of Mo but not Ta. Thus, while the strain fields of the screw dislocations in Mo and Ta are congruent, the connections between atoms are different. The atoms at the dislocation core of Ta are deficient in two bonds, with only six, while Mo has the full complement of eight, as in the bulk.

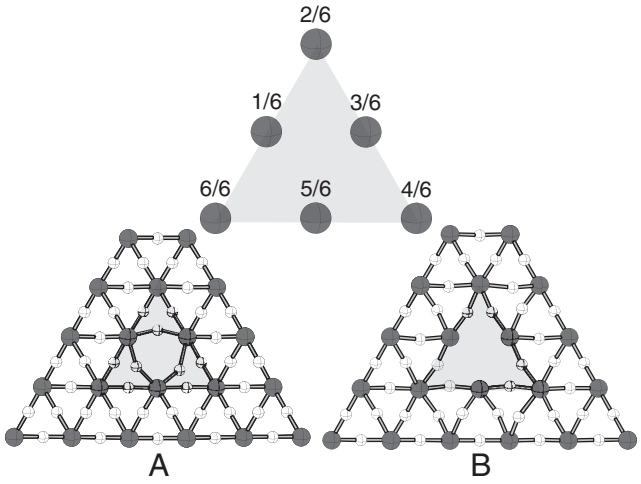

FIG. 1. A projection onto the (111) plane of stress free Mo (A) and Ta (B) cores. Solid spheres give atom positions and open spheres are the locations of bond critical points. Bond paths are shown with connecting lines. The core regions are shaded with triangles. Bonds paths are present across the Mo core, but absent in Ta. Outside the core region the topologies of the two metals are identical. The insert (top) shows the fractional displacement of the atoms in the z direction (in and out of the page) for the atoms immediately adjacent to the core. Any full circuit around the dislocation results in a translation along z equal to one Burgers vector.

Consider now the atoms labeled $1/6$, $3/6$, and $5/6$ in Fig. 1. They are characterized by four bound atoms on an equatorial plane, with the remaining four near neighbor atoms situated on two perpendicular axial planes (see Fig. 2). For the sake of clarity, we define a reference frame with an origin coincident with the $5/6$ atom. The z axis lies along a $\langle 110 \rangle$ direction and passes through the center of the dislocation. This axis is normal to the (110) equatorial plane containing the x and y axes of the local reference frame. One may decompose the charge density into its contributions from all the atomic orbitals and find that with respect to the reference frame, the d_{xy} orbital on the central metal atom (Mo or Ta at the $5/6$ position) contributes density to the bond paths in the equatorial plane. In the case of Mo, the d_{xz} and d_{yz} orbitals contribute density to the bond paths above and below this plane. While for Ta, without bond paths above the plane, there is almost no contribution to the total charge density from the d_{xz} orbital of the central metal atom.

In Ta, symmetry breaking provides the driving force for occupying the d_{yz} at the expense of the d_{xz}. For Mo, the symmetry of the charge density about the $5/6$ atom is nearly D_{2d}—by virtue of an improper fourfold rotation about the z axis (see caption Fig. 2). Under this symmetry, the d_{xz} and d_{yz} orbitals will be nearly degenerate. The projected density of states for the Mo dislocation core confirms this fact, with a nearly full d band derived from the d_{xz} and d_{yz} orbitals of the $1/6$, $3/6$, and $5/6$ type atoms. In the case of Ta, this band would be half full, but is split into an occupied and unoccupied portion. The disappearance of the bond points above the plane lowers the symmetry to nearly C_{2v} and splits the band. The key here is that

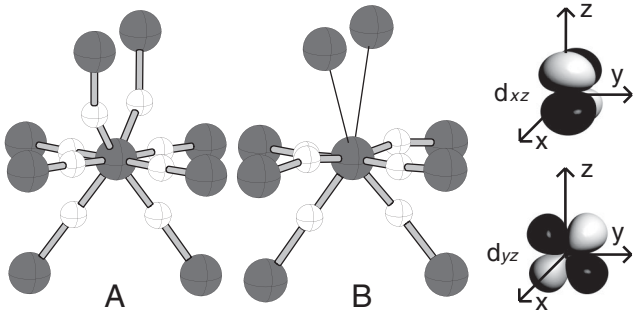

FIG. 2. Structure around Mo (A) and Ta (B) core atoms corresponding to those labeled $1/6$, $3/6$, and $5/6$ in Fig. 1. For Mo, the symmetry of the charge density about the central atom is nearly D_{2d}—a rotation by 90° about the z axis followed by a reflection in the xy plane will carry the bond critical points above the plane into those below the plane. Under this symmetry, the d_{xz} orbitals, which participate in the bonding above the xy plane, are nearly degenerate with the d_{yz} atomic orbitals, which form the two bonds below the plane. In Ta, the absence of bond critical points above the plane reduces the symmetry of the charge density to C_{2v}, lifting the degeneracy between the d_{xz} and d_{yz} atomic orbitals.

in Mo the d_{xy}, d_{xz}, and d_{yz} orbitals are split into two groups, a degenerate pair (d_{xz} and d_{yz}) and an orbital singlet (d_{xy}), while in Ta they are split into three nondegenerate groups.

Consider now the charge redistribution that must accompany dislocation motion. In the bulk, where the local coordination is cubic, the d_{xy}, d_{xz}, and d_{yz} atomic orbitals will be degenerate. As the dislocation moves, and the atoms at the core rearrange to form bulk, degeneracy is achieved through the flow of electrons between them. In turn, this charge redistribution is permitted through the coupling of the charge by the perturbation acting on the dislocation, in this case, the applied strain. The quantum mechanical laws governing this coupling can be reduced to their principal factors by assuming the applied strain rate is slow, with the atoms of the dislocation core moving on an adiabatic potential surface. Then, we can write the strain perturbation as a sum of two static parts: a term that depends only on the strain and one that depends on its spatial rate of change, i.e.,

$$\varepsilon(\vec{r} + d\vec{r}) \approx \varepsilon(\vec{r}) + d\vec{r} \cdot \nabla\varepsilon(\vec{r}), \tag{1}$$

where ε is the strain. The second term on the right is simply the rate of change of the strain in the direction $d\vec{r}$. This term will be zero in a material with uniform elastic properties. In a material with varying elastic properties, however, it will change most rapidly along the directions in which bonds are being made and broken due to the strain at r—the first term on the right. Thus, each of these terms can couple orbitals and facilitate charge redistribution; their importance in this process, however, will be determined by their relative magnitudes.

The results summarized in Ref. [5] confirm that for both Ta and Mo dislocations moving under a twinning stress the magnitudes of the two terms in Eq. (1) are comparable, for as the strain is applied, new bonds form and the dislocation moves at a small Peierls strain. On the other hand, in the antitwinning sense, bond breaking and making occurs late in the reaction coordinate (large Peierls strain) and only after significant atomic rearrangement. Hence, for antitwinning, the initial response of the dislocations is dominated by the applied strain. And, whereas the quantum mechanical constraints imposed on the charge redistribution are difficult to predict when $d\vec{r} \cdot \nabla\varepsilon(\vec{r})$ is large, when it is small or vanishes (antitwinning stresses), we can call upon the principles of symmetry to predict the atomic motions that couple orbitals and permit charge flow. (See the supporting material at end.)

Beginning with Mo, charge flow between the d_{xz}-d_{yz} pair and the d_{xy} orbital is only permitted when atoms move in response to a shear stress in the (110) plane. On the other hand, in Ta, with three singly degenerate orbitals, there are two coupling strains. The empty d_{xz} orbital is coupled to the occupied d_{yz} orbital by shear strains lying in a plane perpendicular to the (110) plane. Shear strains in the (110) plane couple the remaining orbitals—d_{xy} to d_{xz} and d_{xy} to d_{yz}. The constraints imposed by these coupling rules, known formally as selection rules, are seen as Ta and Mo deform under an antitwinning stress.

As a rule, dislocations in metals move along close-packed planes. Thus, in bcc metals, dislocations are expected to move along {110} planes, which is the case for Mo. For example, when a pure shear stress is applied in the $\langle 111 \rangle$ antitwinning sense, dislocations in Mo move as expected (along the (110) plane of maximum resolved shear stress) [5,7,12,13]. In Ta, however, the dislocation responds to this shear stress on the (112) plane [5,7,14,15]. Only after significant charge redistribution can bonds begin to form, at which point the dislocation propagates in response to the gradient terms of Eq. (1). Thus, the driving force for the motion is the formation of bonds using tantalum's empty d_{xz} orbital. The charge to form these bonds comes from electrons in the Ta d_{yz} orbital. This charge flow is not allowed if the dislocation is confined to the (110) plane but is possible by coupling orbitals through the strain field in the (112) plane. The observed motion of dislocations in Ta under antitwinning stress is consistent with the symmetry imposed selection rules. Ultimately, these differences stem from the fact that Ta has one fewer valence electron than does Mo.

Because the differences between Ta and Mo can be traced to electron count, we speculate that Nb and W will have core structures similar to Ta and Mo, respectively. However, the degree of $s - d$ hybridization changes within a Group and could result in subtle differences in dislocation core bonding within a Group. Hence, a definitive test of this speculation must await more calculations.

With an electronic mechanism for dislocation motion in hand, the effects of dilute substitutional impurities in bcc metals are predictable. Substitutional alloying of elements to the left of the Group V metals will deplete the d band, yielding an alloy with properties more like those of Ta. Conversely, those to the right will further fill the d band, producing properties more like Mo, a trend recovered using DFT methods [16]. This result is entirely reasonable based on purely empirical arguments.

Combining DFT with the topological model of molecular bonding, we were able to uncover structure-property relationships that have eluded others. The procedure used here should be equally applicable to problems of fracture and deformation where empirical findings do not provide guidance. For example, the Mott and Nabarro [17] theory of low-temperature solute hardening requires as a parameter the breakaway energy for a dislocation pinned by a solute atom—a parameter that is difficult to measure. As we have argued, this energy will be governed through the quantum mechanical interactions between the dislocation core and the solute atom and thus cannot be calculated by traditional means. However, once determined with quantum methods, the value can be used as a parameter within

the Mott-Nabarro model to give guidance as to the concentration dependence of solutes on hardening or softening. The future is one where integrated classical and quantum mechanical models will be necessary to rationalize and predict the properties of materials, and the approach presented here represents a step toward achieving this integration.

Supporting material.—With respect to the D_{2d} point group, the d_{xz} and d_{yz} atomic orbitals transform as the doubly degenerate E representation, while the d_{xy} orbital transforms as the irreducible representation B_2. If we take Γ_v to be the irreducible representation of the strains that couple these two, then the fully symmetric representation, A_1, must be contained in the direct product of $E \times \Gamma_v \times B_2$. From which one may show that Γ_v transforms as E, which possess the same symmetry as shear strains in the (110) plane. With respect to the C_{2v} point group, d_{yz} reduces as B_2, d_{xz} as B_1 and d_{xy} as A_2. Knowing that $B_2 \times B_1 \times A_2 = A_1$, it can be shown that: d_{xz} is coupled to d_{yz} by an A_2 strain (shear couple applied in a plane normal to the z axis), d_{xy} is coupled to d_{yz} by a B_1 strain (shear normal to the y axis), and d_{xy} is coupled to d_{xz} by a B_2 strain (shear couple normal to the y axis). B_1 and B_2 form a symmetry basis for the full set of shear strains in the (110) plane of Fig. 2.

We are grateful to the Defense Advanced Projects Agency and the Office of Naval Research for their support of this research.

*trjones@mines.edu
+meberhar@mines.edu

[1] V. Vitek, Cryst. Lattice Defects **5**, 1 (1974).
[2] C. Woodward and S. I. Rao, Philos. Mag. A **81**, 1305 (2001).
[3] M. S. Duesbery, V. Vitek, and D. K. Bowen, Proc. R. Soc. A **332**, 85 (1973).
[4] W. Xu and J. A. Moiriarity, Phys. Rev. B **54**, 6941 (1996).
[5] M. S. Duesbery and V. Vitek, Acta Mater. **46**, 1481 (1998).
[6] S. Ismail-Beigi and T. A. Arias, Phys. Rev. Lett. **84**, 1499 (2000).
[7] C. Woodward and S. I. Rao, Phys. Rev. Lett. **88**, 216402 (2002).
[8] C. Woodward, Mater. Sci. Eng. A **400–401**, 59 (2005).
[9] P. Hohenberg and W. Kohn, Phys. Rev. **136**, B864 (1964).
[10] R. F. W. Bader, *Atoms in Molecules. A Quantum Theory* (Clarendon Press, Oxford, UK, 1990).
[11] P. F. Zou and R. F. W. Bader, Acta Crystallogr. Sect. A **50**, 714 (1994).
[12] D. Vesely, Phys. Status Solidi **29**, 675 (1968).
[13] P. Sherwood, F. Guiu, H. Kim, and P. Pratt, Can. J. Phys. **45**, 1075 (1967).
[14] S. Takeughi, E. Kuramoto, and T. Suzuki, Acta Metall. **20**, 909 (1972).
[15] M. Nawaz and B. Mordike, Phys. Status Solidi **32**, 449 (1975).
[16] D. R. Trinkle and C. Woodward, Science **310**, 1665 (2005).
[17] N. Mott and F. Nabarro, Proc. Phys. Soc. London **52**, 86 (1940).